Estágios da formação estelar

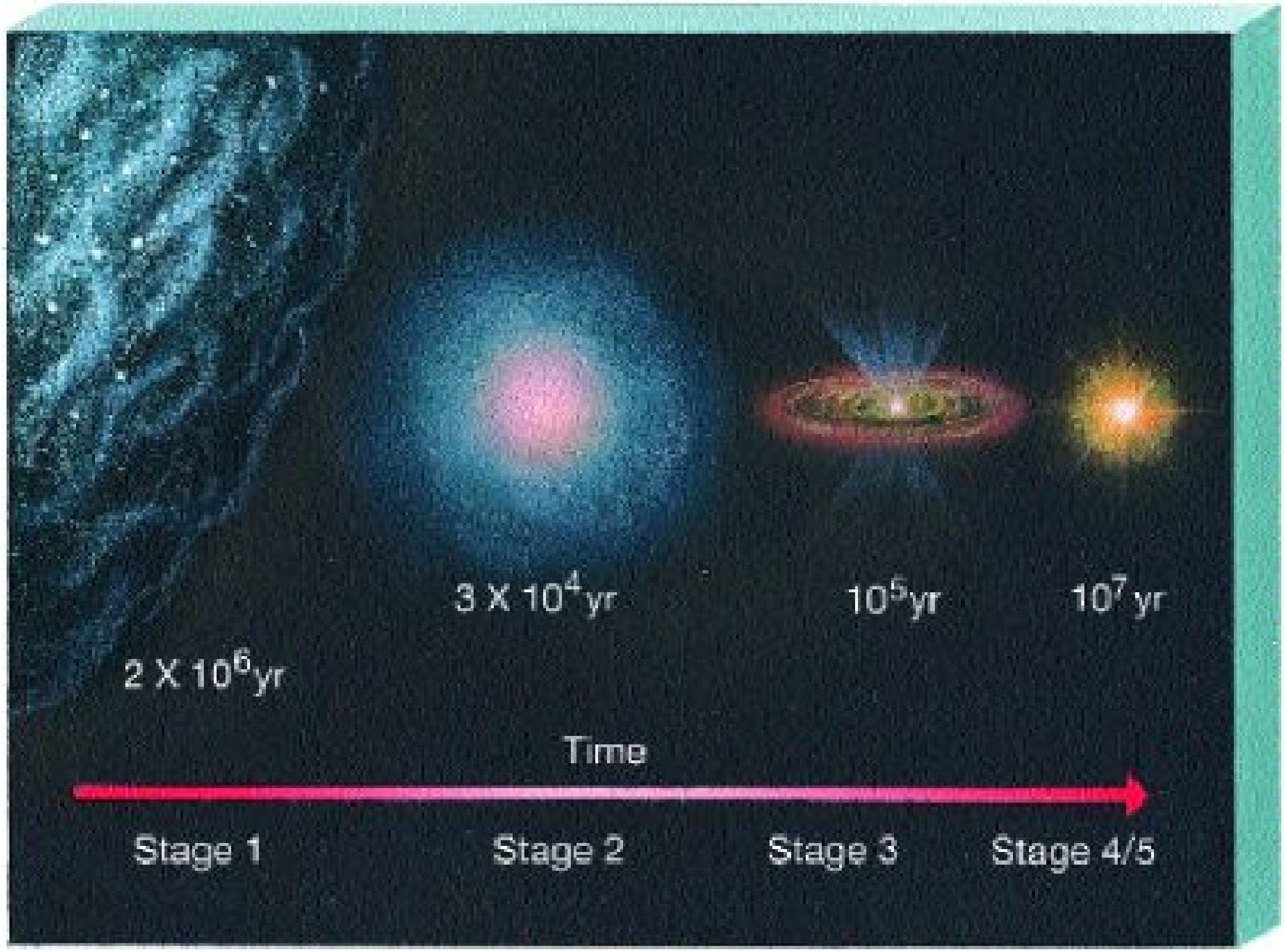

1 - Colapso nuvem de gás;
2 - Proto-estrelas;
3 - Pré-sequência principal

Etapas da Formação Protoestelar

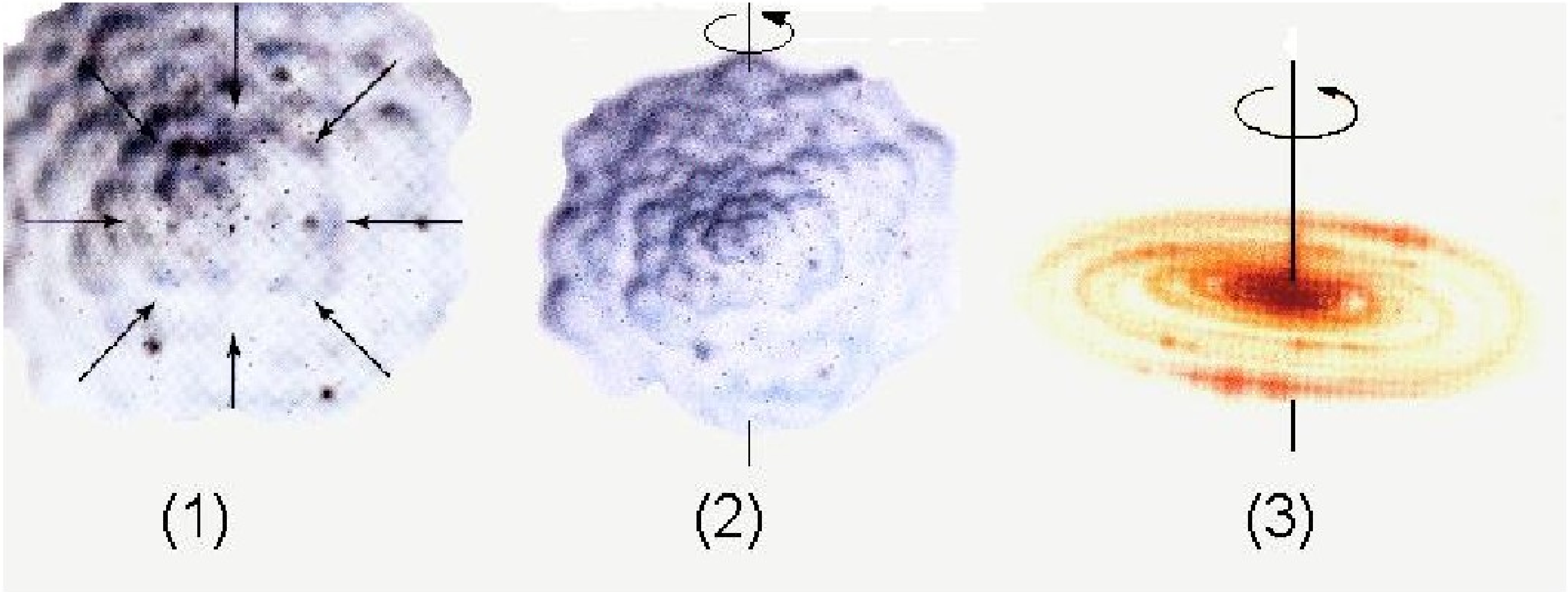

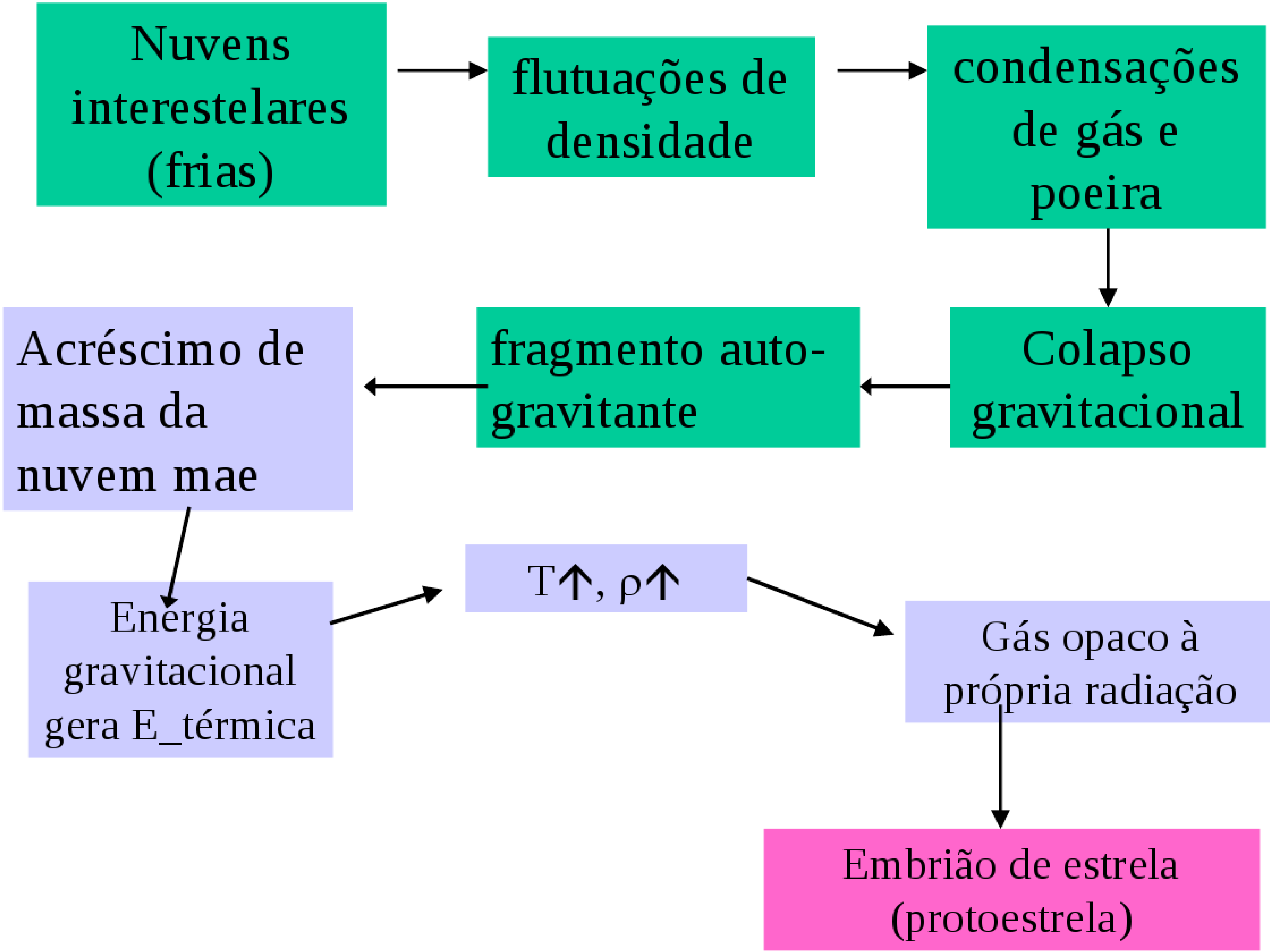
Nuvens interestelares (frias)
flutuações de densidade
condensações de gás e poeira
Colapso gravitacional
fragmento auto-gravitante
Acréscimo de massa da nuvem mae
Energia gravitacional gera E_térmica
T↑, ρ↑
Gás opaco à própria radiação
Embrião de estrela (protoestrela)

Star Formation

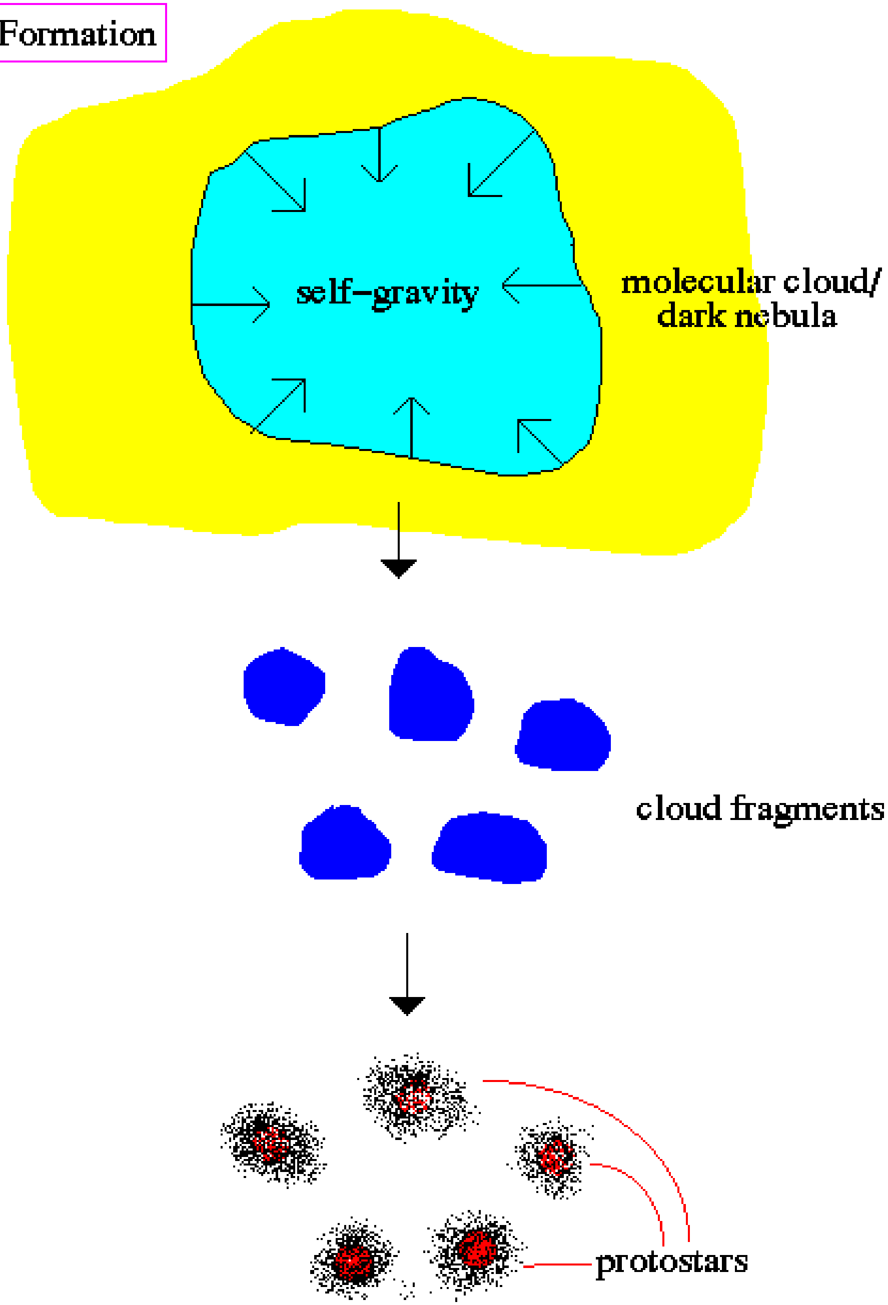

Protostar Formation

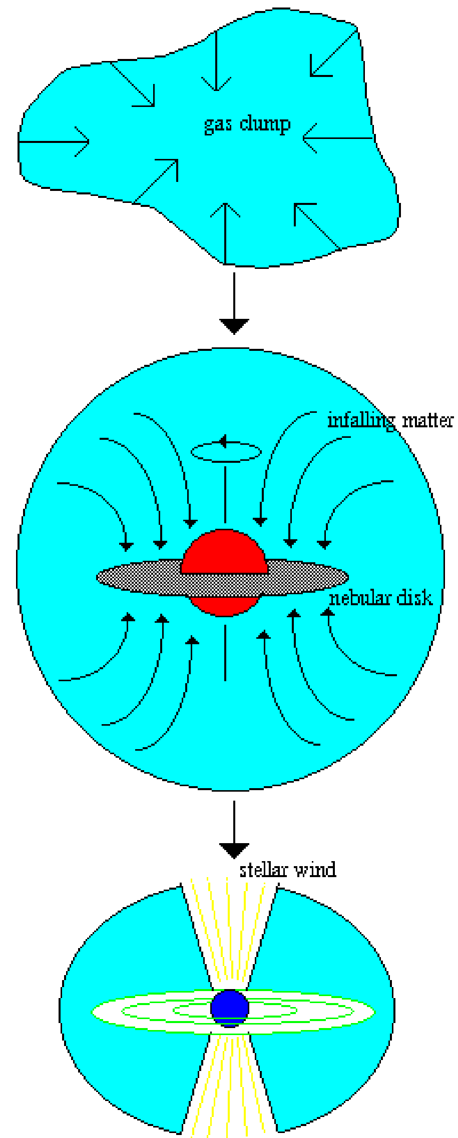

A dense gas clump breaks off from molecular cloud and collapses Angular momentum turns the irregular clump into a rotating disk

The central region is denser and forms into a protostar, the nebular disk forms slower to become a planetary system. Infalling matter increases the size of the protostar by a factor of 100

Infall is stopped when the protostar begins thermonuclear fusion and produces a strong stellar wind

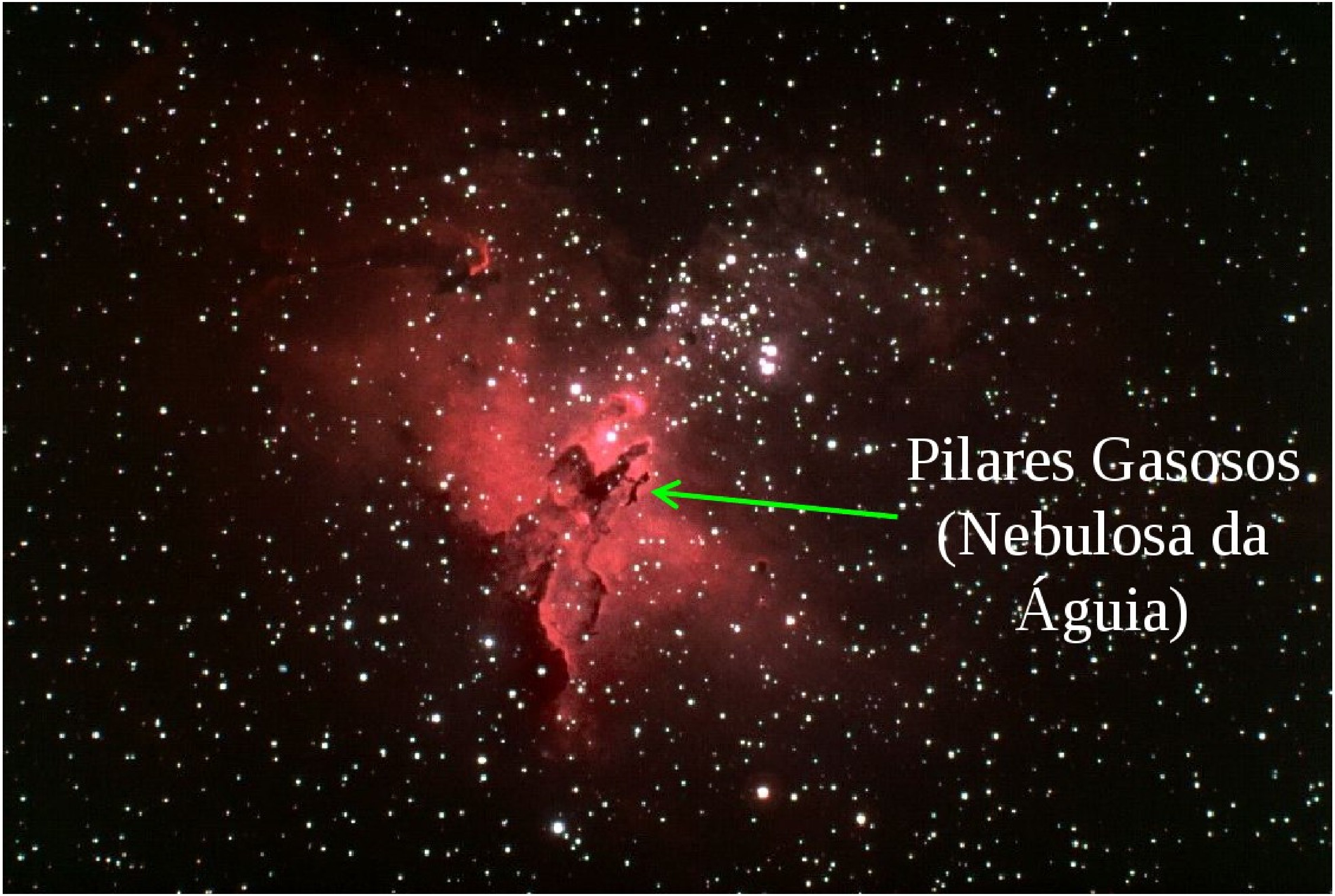
Pilares Gasosos
(Nebulosa da
Águia)

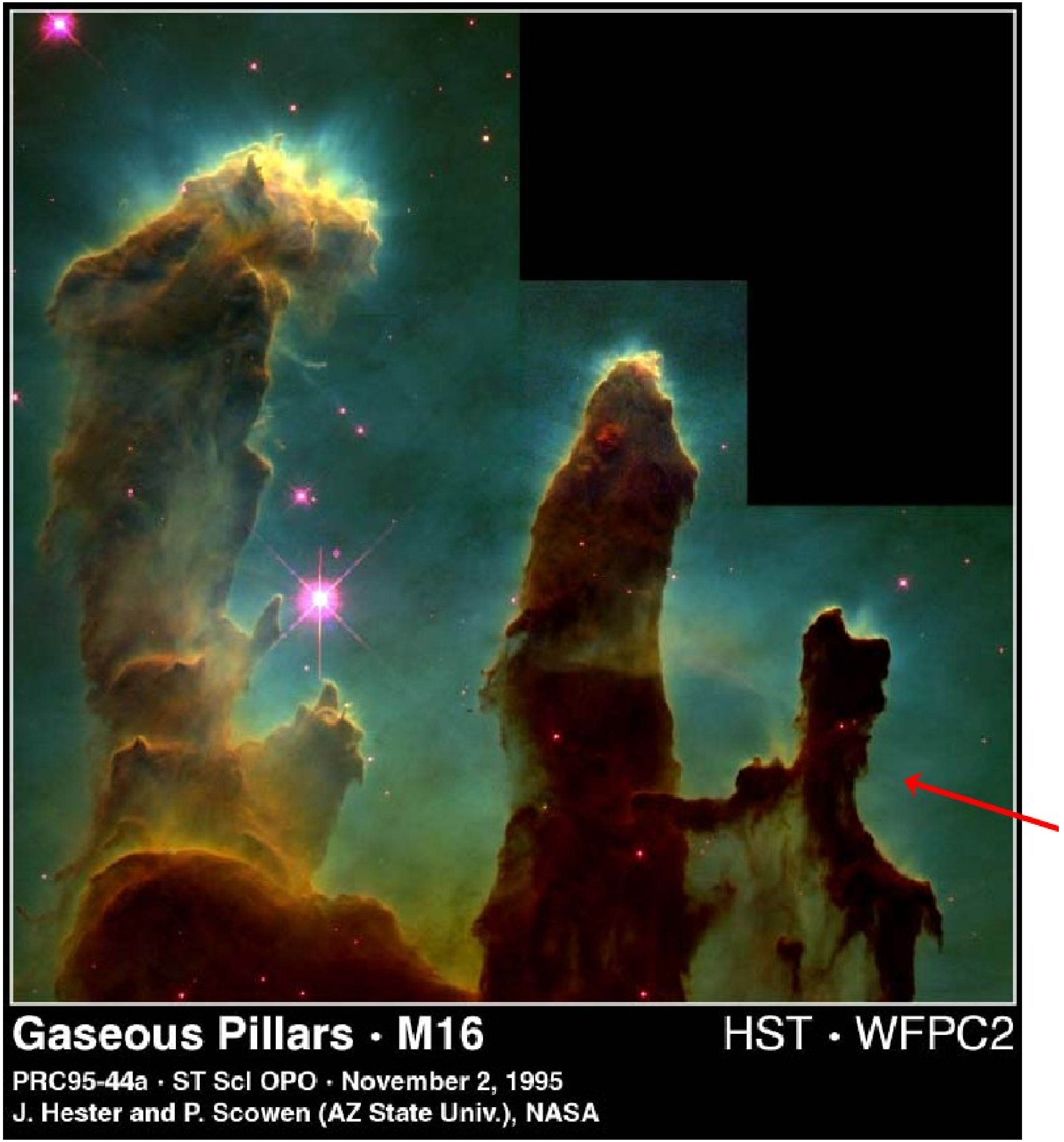
Gaseous Pillars · M16
HST · WFPC2
PRC95-44a · ST ScI OPO · November 2, 1995
J. Hester and P. Scowen (AZ State Univ.), NASA

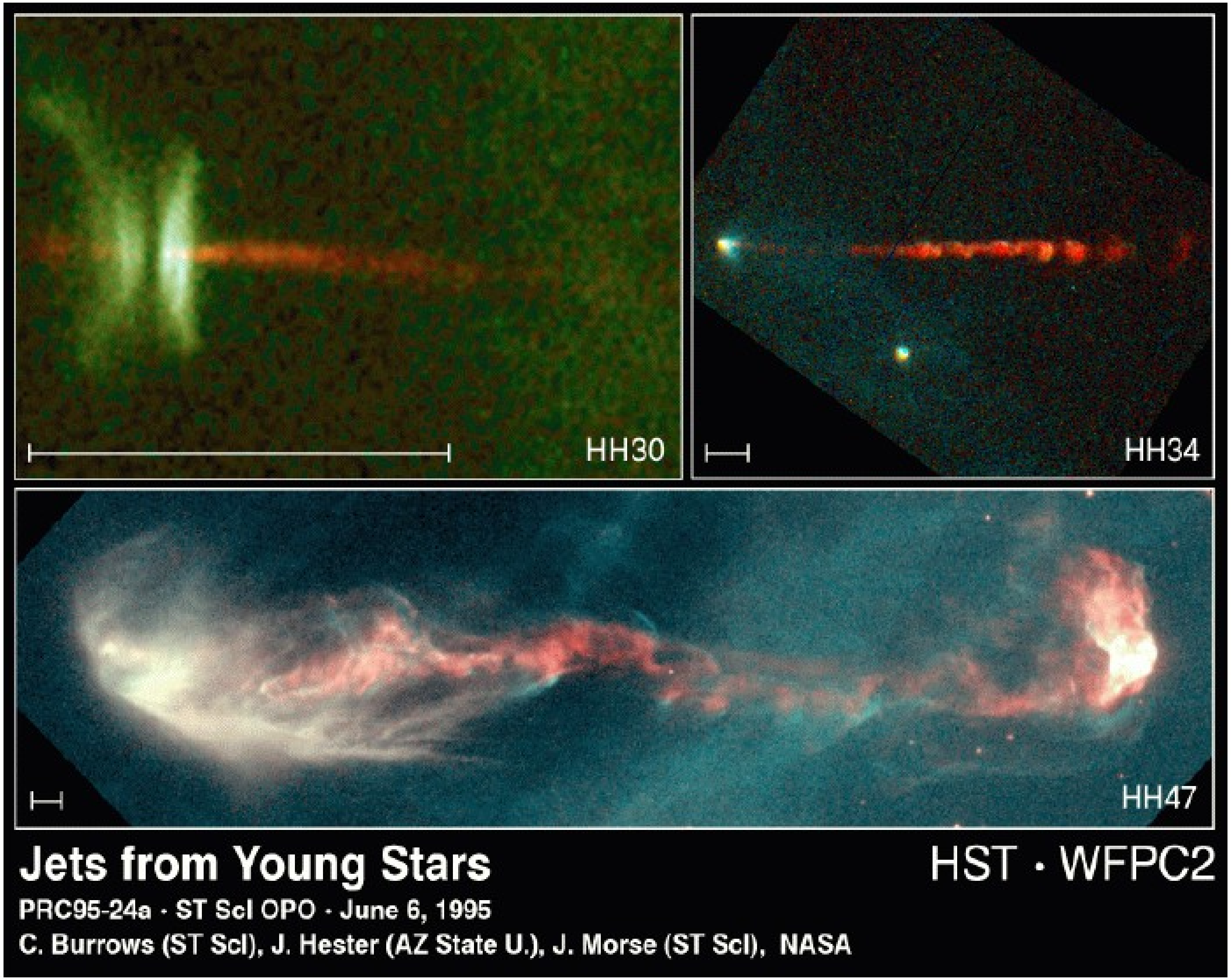
HH30
HH34
HH47
Jets from Young Stars
HST · WFPC2
PRC95-24a · ST ScI OPO · June 6, 1995
C. Burrows (ST ScI), J. Hester (AZ State U.), J. Morse (ST ScI), NASA

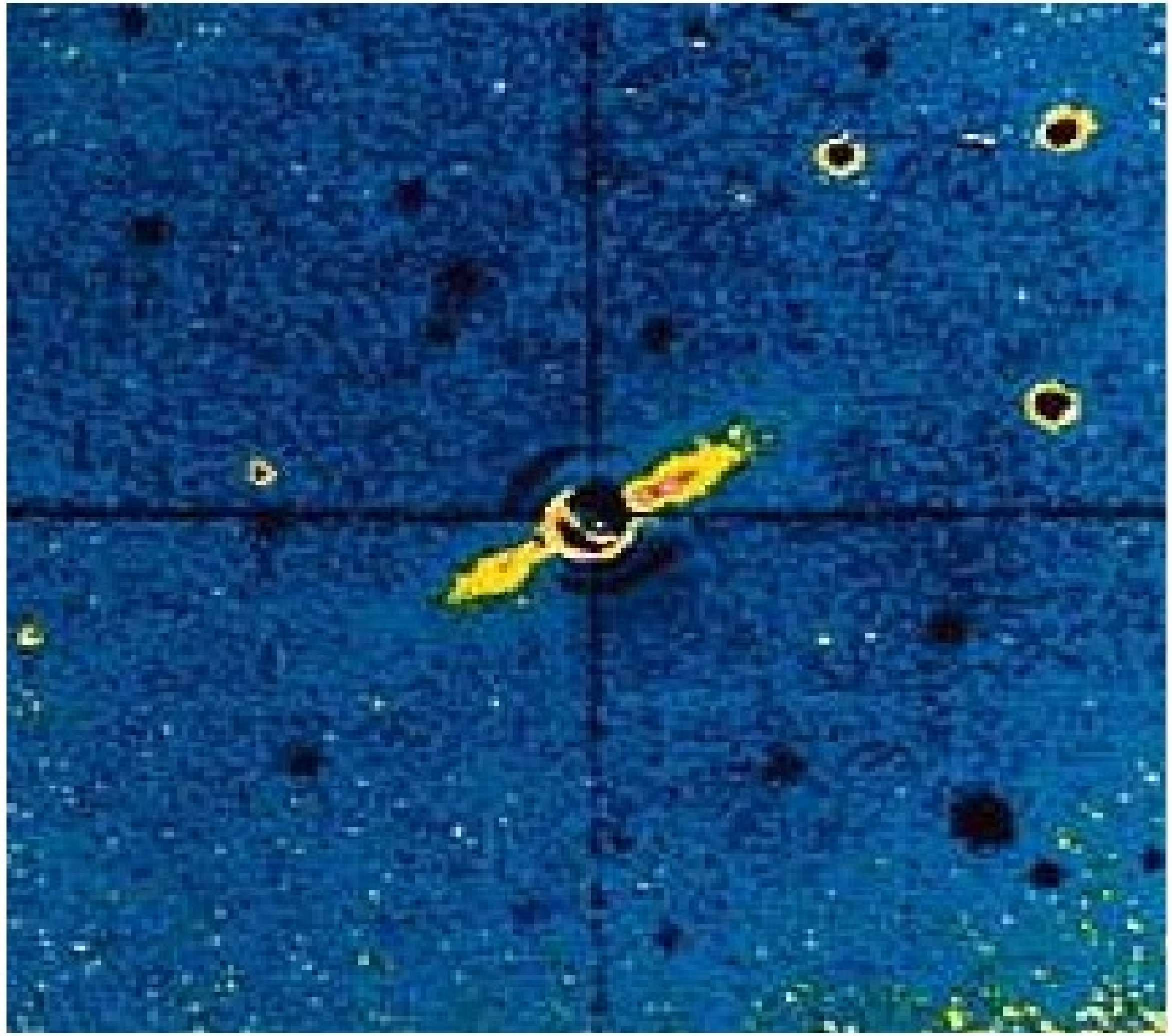

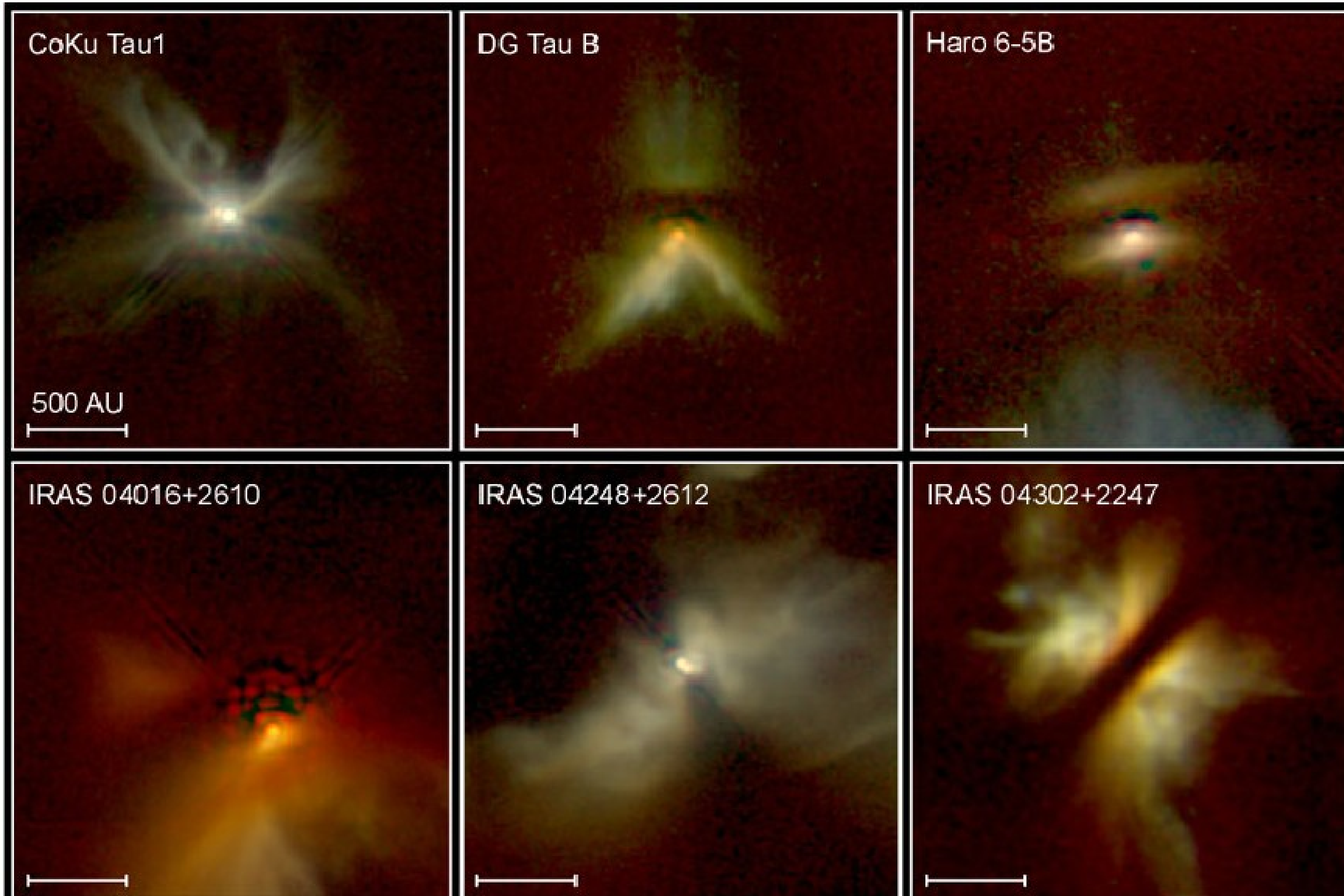

Young Stellar Disks in Infrared **HST • NICMOS**

PRC99-05a • STScI OPO

D. Padgett (IPAC/Caltech), W. Brandner (IPAC), K. Stapelfeldt (JPL) and NASA

Gravidade versus Pressão
Papel central: Opacidade

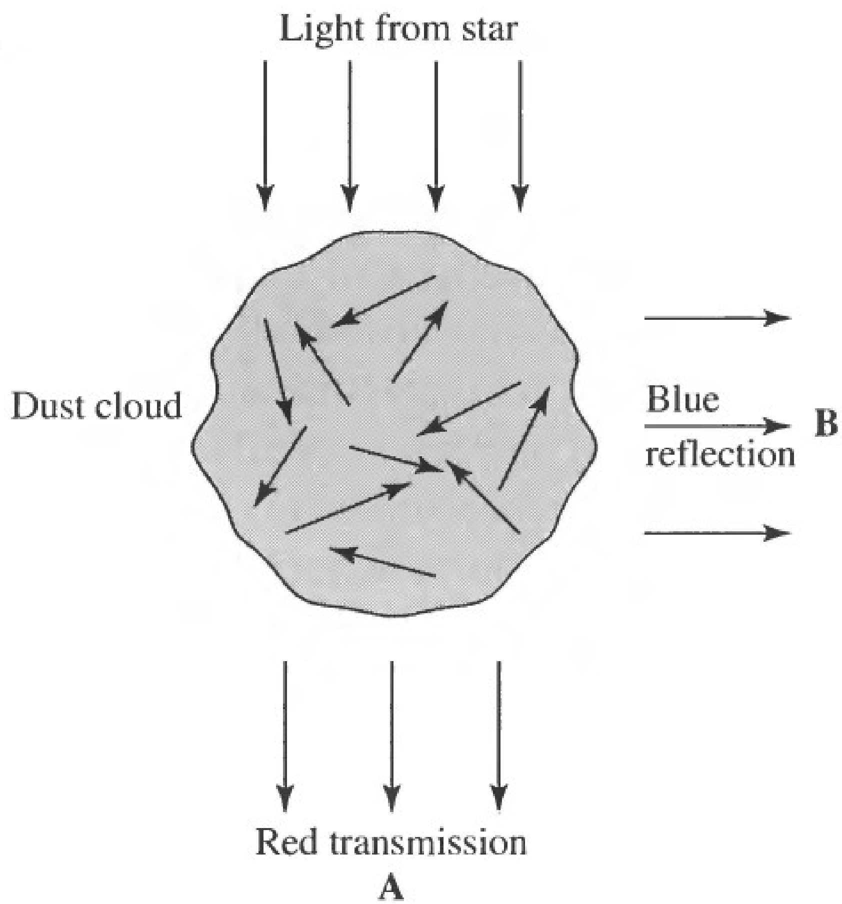

Critério de Jeans

$$2K + U = 0, \qquad U \sim -\frac{3}{5}\frac{GM_c^2}{R_c}, \qquad K = \frac{3}{2}NkT,$$

Condição para colapso: $(2K < |U|)$

$$\frac{3M_c kT}{\mu m_H} < \frac{3}{5}\frac{GM_c^2}{R_c}. \qquad R_c = \left(\frac{3M_c}{4\pi\rho_0}\right)^{1/3}.$$

Massa de Jean

Massa necessária para colapso

$$M_J \simeq \left(\frac{5kT}{G\mu m_H}\right)^{3/2}\left(\frac{3}{4\pi\rho_0}\right)^{1/2}$$

Tempo de queda livre

$$\frac{d^2r}{dt^2} = -\frac{GM(r)}{r^2}$$

$$v^2 = \frac{8\pi G\rho_0}{3}\int_0^r r\,dr = \frac{4\pi G\rho_0}{3} r^2$$

$$t_{ff} = \left(\frac{3\pi}{32}\frac{1}{G\rho_0}\right)^{1/2}.$$

$\mathbf{v} \propto \mathrm{r}$

Não depende do raio -> Colapso homólogo

Example 12.2.2. Using data given in Example 12.2.1 for a dense core of a giant molecular cloud, we may estimate the amount of time required for the collapse. Assuming a density of $\rho_0 = 3 \times 10^{-17}\ \mathrm{kg\ m^{-3}}$ that is constant throughout the core, Eq. (12.26) gives

$$t_{ff} = 3.8 \times 10^5\ \mathrm{yr}.$$

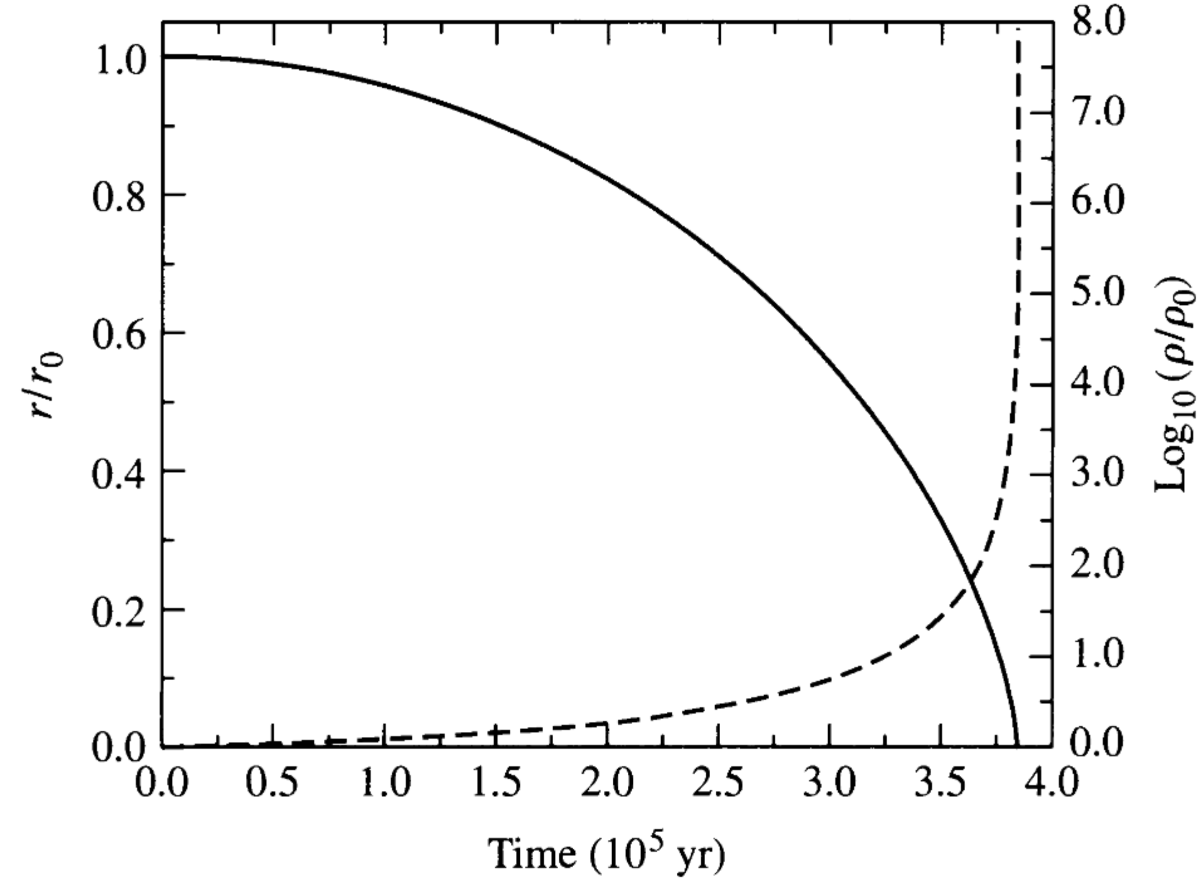

FIGURE 12.8 The homologous collapse of a molecular cloud, as discussed in Example 12.2.2. r/r_0 is shown as the solid line and $\log_{10}(\rho/\rho_0)$ is shown as the dashed line. The initial density of the cloud was $\rho_0 = 3 \times 10^{-17}$ kg m^{-3} and the free-fall time is 3.8×10^5 yr.

The Rotational Energy The Virial theorem can also be used to determine the effects of rotation on a collapsing cloud. Again, from Chapter 1, the rotational kinetic energy must be less than one-half the gravitational potential energy in order for the cloud to collapse. So

$$2\left(\tfrac{1}{2}I\omega^2\right) \leq \frac{GM^2}{R_c} \tag{5.2.3}$$

which for a sphere of uniform density and constant angular velocity gives

$$R_c \leq \left(\frac{5GM}{2\omega^2}\right)^{1/3} \tag{5.2.4}$$

The differential rotation of the galaxy implies that there must be a shear or velocity gradient which would impart a certain amount of rotation to any dynamical entity forming from the interstellar medium. For an Oort constant, A = 16 km/s/kpc, this implies that

$$R_c \leq 0.9\left(\frac{M}{M_\odot}\right)^{1/3} \quad \text{pc} \tag{5.2.5}$$

Thus, it would seem that to quell rotation, the initial mass of the sun must have been confined within a sphere of about 0.7 pc.

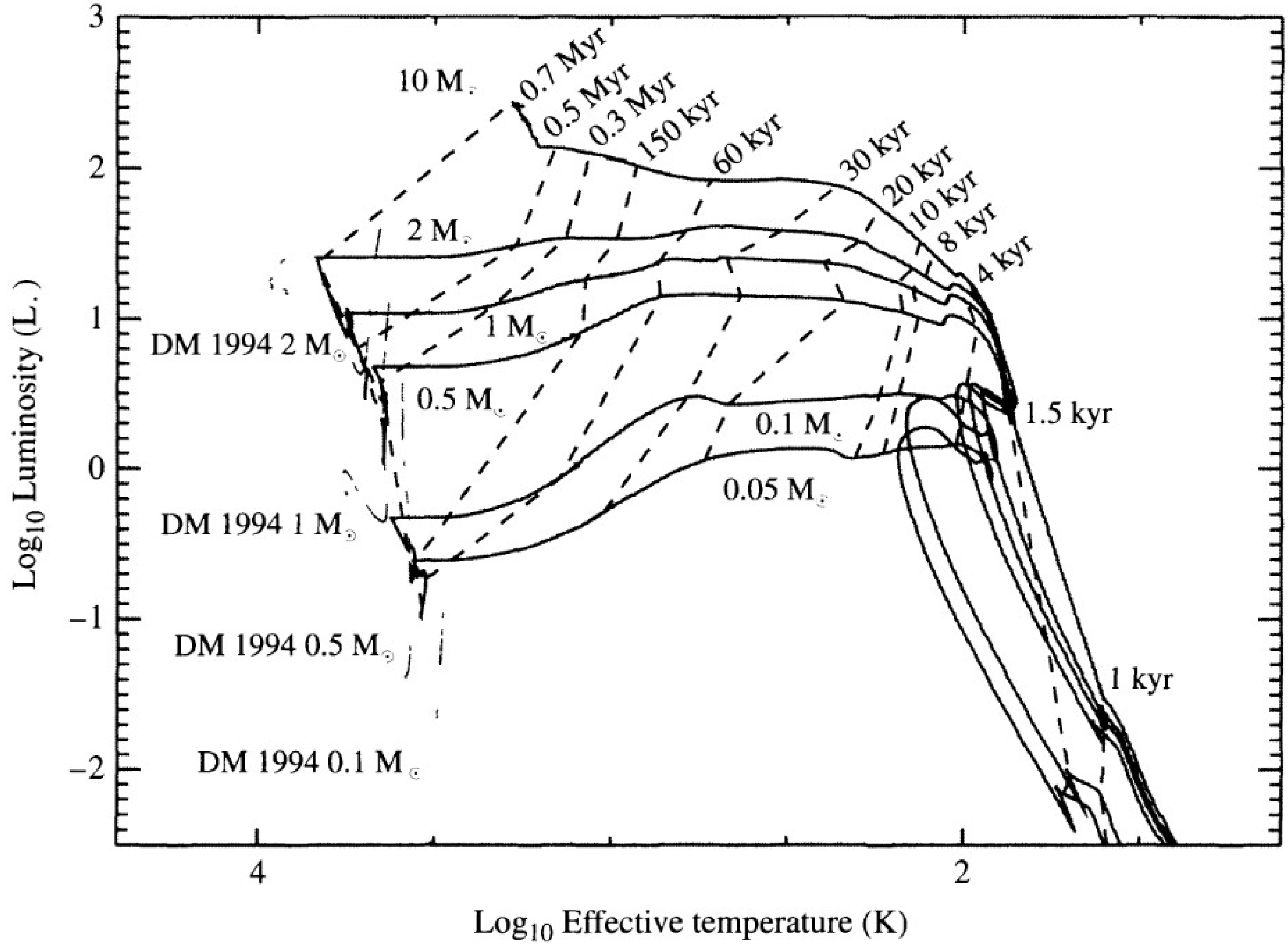

FIGURE 12.9 Theoretical evolutionary tracks of the gravitational collapse of 0.05, 0.1, 0.5, 1, 2, and 10 $M_\odot$ clouds through the protostar phase (solid lines). The dashed lines show the times since collapse began. The light dotted lines are pre-main-sequence evolutionary tracks of 0.1, 0.5, 1, and 2 $M_\odot$ stars from D'Antona and Mazzitelli, *Ap. J. Suppl.*, *90*, 457, 1994. Note that the horizontal axis is plotted with effective temperature increasing to the left, as is characteristic of all H–R diagrams. (Figure adapted from Wuchterl and Tscharnuter, *Astron. Astrophys.*, *398*, 1081, 2003.)

Pré-sequência principal

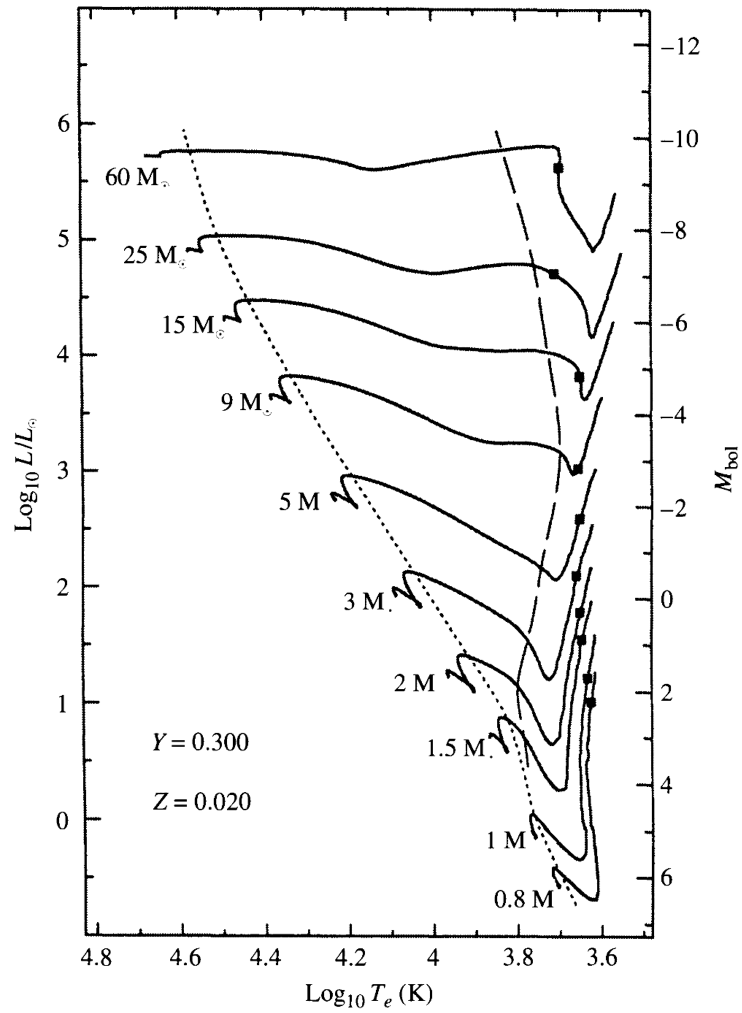

FIGURE 12.11 Classical pre-main-sequence evolutionary tracks computed for stars of various masses with the composition $X = 0.68$, $Y = 0.30$, and $Z = 0.02$. The direction of evolution on each track is generally from low effective temperature to high effective temperature (right to left). The mass of each model is indicated beside its evolutionary track. The square on each track indicates the onset of deuterium burning in these calculations. The long-dash line represents the point on each track where convection in the envelope stops and the envelope becomes purely radiative. The short-dash line marks the onset of convection in the core of the star. Contraction times for each track are given in Table 12.1. (Figure adapted from Bernasconi and Maeder, *Astron. Astrophys.*, *307*, 829, 1996.)

TABLE 12.1 Pre-main-sequence contraction times for the classical models presented in Fig. 12.11. (Data from Bernasconi and Maeder, *Astron. Astrophys.*, *307*, 829, 1996.)

Initial Mass ($M_\odot$)	Contraction Time (Myr)
60	0.0282
25	0.0708
15	0.117
9	0.288
5	1.15
3	7.24
2	23.4
1.5	35.4
1	38.9
0.8	68.4

1 - Colapso gravitacional
2 - Apenas primeiro estágio da cadeia PP1 acontece -> diminui a velocidade do colapso
3 - Temperatura segue aumentando, núcleo ionizado e radiativo, energia escapa pra superfície, pode ocorrer jatos.
4 - Estágio 2 e 3 da cadeia PP1 e primeiro estágio da cadeia CNO são ativados
5 - Excesso de energia nuclear -> aumento da pressão -> aumento do raio -> diminuição da temperatura
6,7 - Cadeia PP1 completa se instaura

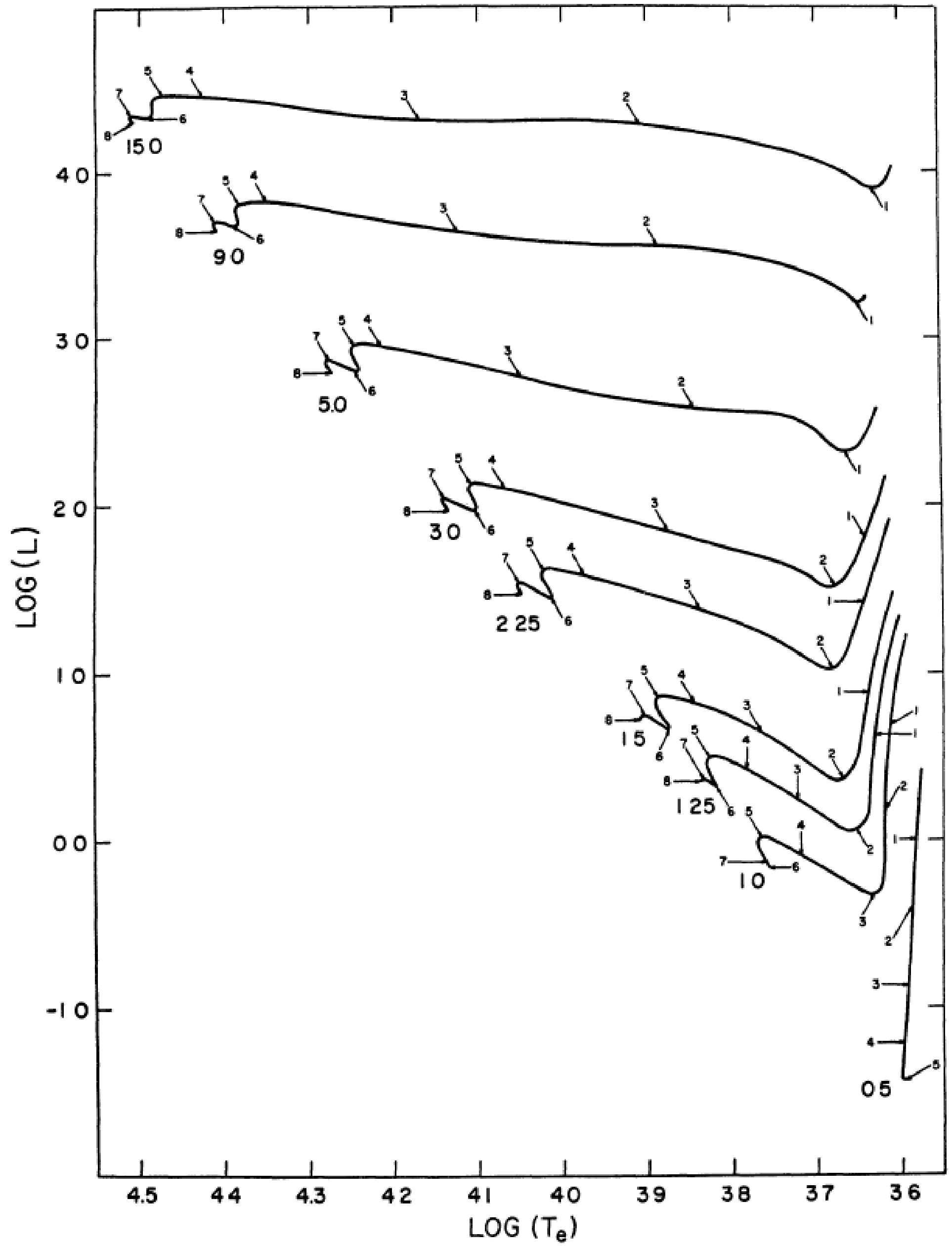

FIG. 17.—Paths in the Hertzsprung-Russell diagram for models of mass ($M/M_\odot$) = 0.5, 1.0, 1.25, 1.5, 2.25, 3 0, 5.0, 9.0, and 15.0. Units of luminosity and surface temperature are the same as those in Fig. 1

Evolutionary Lifetimes

Point	$(M/M_\odot)$								
	15.0	9.0	5.0	3.0	2.25	1.5	1.25	1.0	0.5
1	6.740×10^{2}	1.443×10^{3}	2.936×10^{4}	3.420×10^{4}	7.862×10^{4}	2.347×10^{5}	4.508×10^{5}	1.189×10^{5}	3.195×10^{5}
2	3.766×10^{3}	1.473×10^{4}	1.069×10^{5}	2.078×10^{5}	5.940×10^{5}	2.363×10^{6}	3.957×10^{6}	1.058×10^{6}	1.786×10^{6}
3	9.350×10^{3}	3.645×10^{4}	2.001×10^{5}	7.633×10^{5}	1.883×10^{6}	5.801×10^{6}	8.800×10^{6}	8.910×10^{6}	8.711×10^{6}
4	2.203×10^{4}	6.987×10^{4}	2.860×10^{5}	1.135×10^{6}	2.505×10^{6}	7.584×10^{6}	1.155×10^{7}	1.821×10^{7}	3.092×10^{7}
5	2.657×10^{4}	7.922×10^{4}	3.137×10^{4}	1.250×10^{6}	2.818×10^{6}	8.620×10^{6}	1.404×10^{7}	2.529×10^{7}	1.550×10^{8}
6	3.984×10^{4}	1.019×10^{5}	3.880×10^{5}	1.465×10^{6}	3.319×10^{6}	1.043×10^{7}	1.755×10^{7}	3.418×10^{7}	
7	4.585×10^{4}	1.195×10^{5}	4.559×10^{5}	1.741×10^{6}	3.993×10^{6}	1.339×10^{7}	2.796×10^{7}	5.016×10^{7}	
8	6.170×10^{4}	1.505×10^{5}	5.759×10^{5}	2.514×10^{6}	5.855×10^{6}	1.821×10^{7}	2.954×10^{7}		

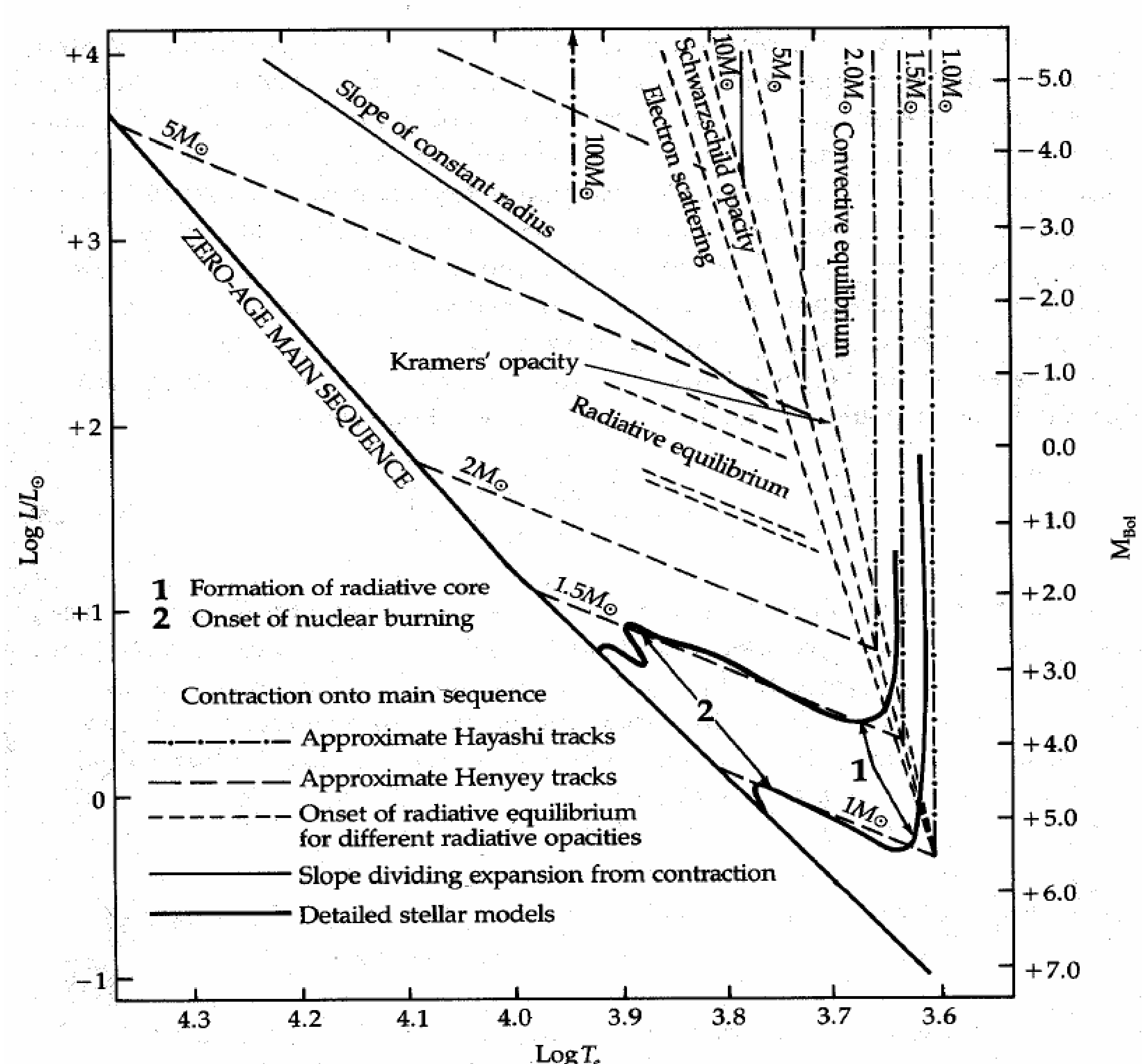

Figure 5.1 shows the schematic tracks for fully convective stars and radiative stars on their way to the main sequence. The low dependence of the convective tracks on mass implies that most contracting stars will occupy a rather narrow band on the right hand side of the H-R diagram. The line of constant radius clearly indicates that stars on the Henyey tracks continue to contract. The dashed lines indicate the transition from convective to radiative equilibrium for differing opacity laws. The solid curves represent the computed evolutionary tracks for two stars of differing mass[5].

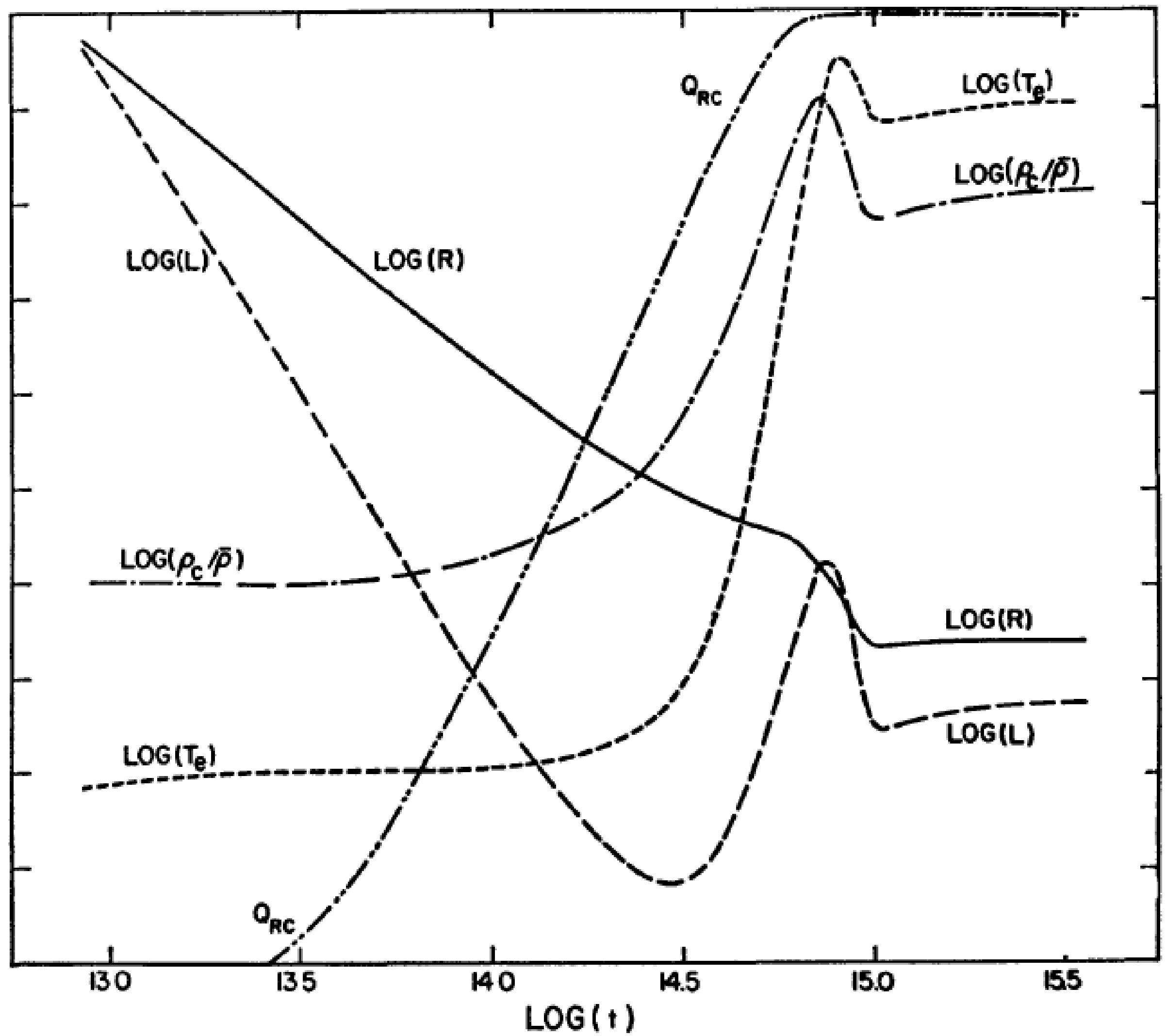

FIG 2—The variation with time t (in sec) of surface temperature T_e (in units of ° K), luminosity L (in units of 3.86×10^{33} erg/sec), stellar radius R (in units of 6.96×10^{10} cm), central over mean density $\rho_c/\bar{\rho}$, and mass fraction in the radiative core Q_{RC} for a stellar model of mass $M = M_\odot$. Maximum and minimum scale limits correspond to: $3.58 < \log T_e < 3.78$, $-0.4 < \log L < 0.6$, $-0.4 < \log R < 0.6$, $0.0 < \log (\rho_c/\bar{\rho}) < 2.0$, and $0 < Q_{RC} < 1$.

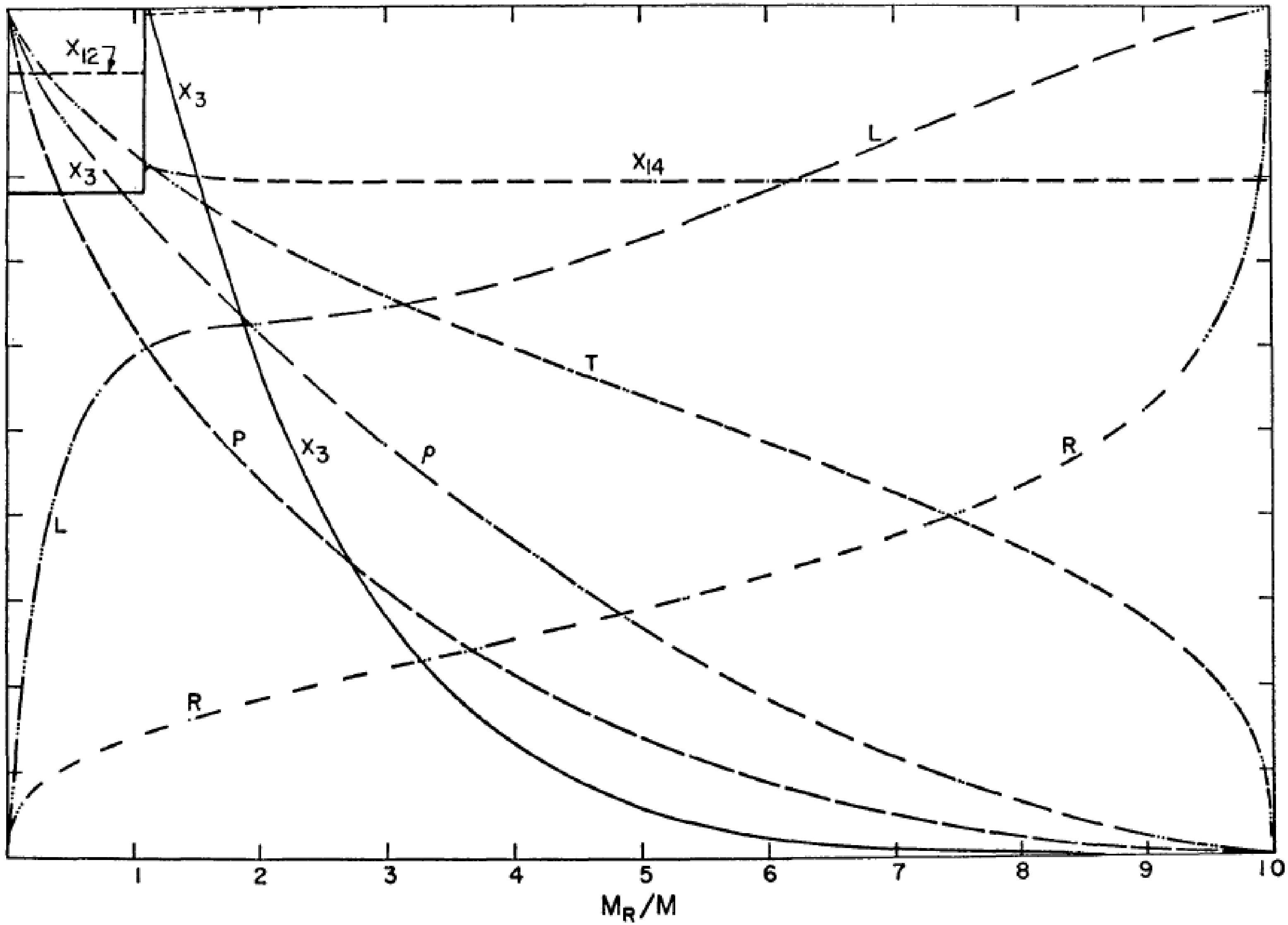

FIG. 4.—The variation with mass fraction of pressure P, temperature (T), density (ρ), luminosity (L), radius (R), He^3 abundance by mass (X_3), C^{12} abundance by mass (X_{12}), and N^{14} abundance by mass (X_{14}). Model mass $M = M\odot$ and log (t) = 14.941. The maximum value of each variable is on the scale of unity. Maximum values in physical units are listed in the first row of Table 2.

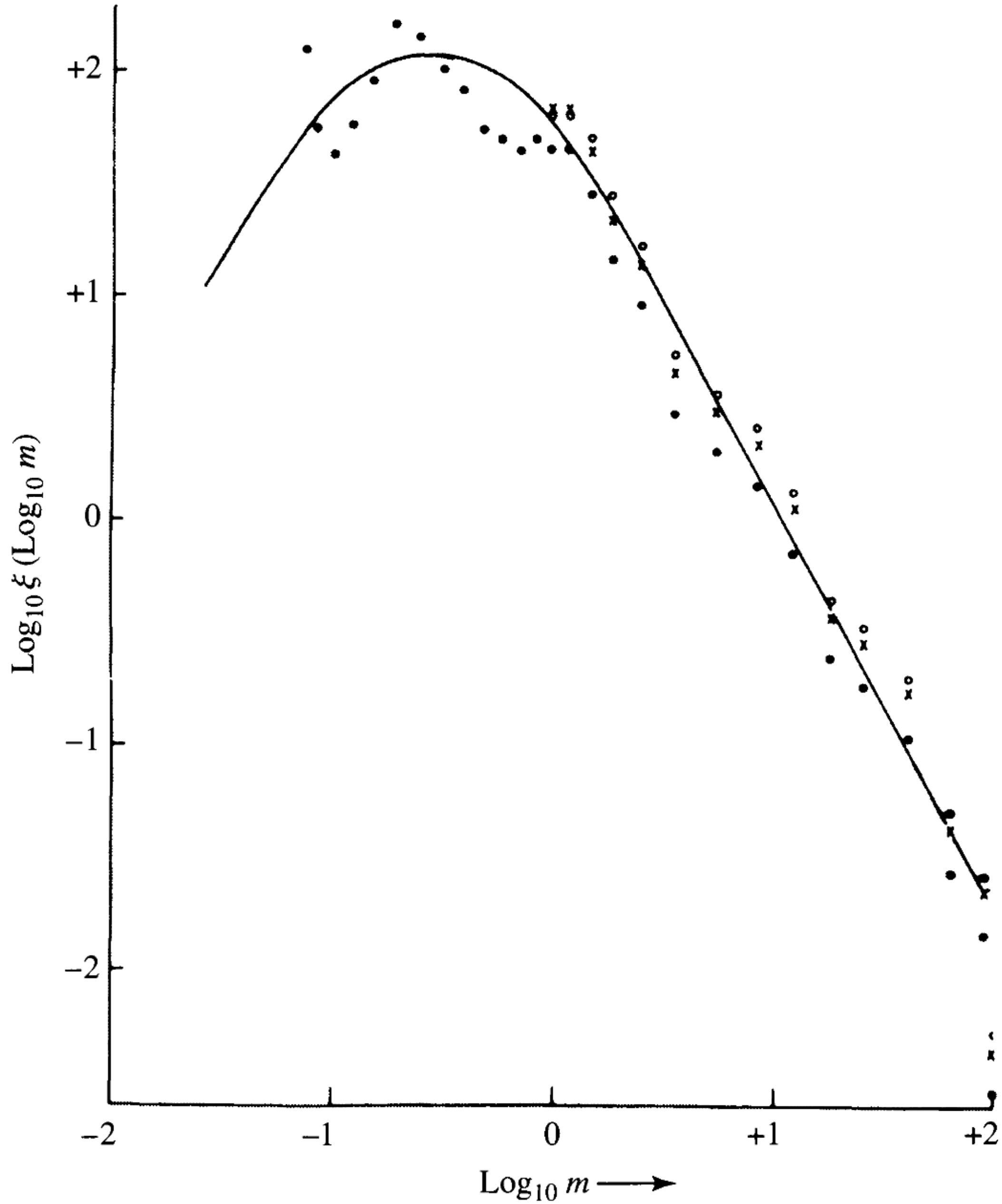

FIGURE 12.12 The initial mass function, ξ, shows the number of stars per unit area of the Milky Way's disk per unit interval of logarithmic mass that is produced in different mass intervals. The individual points represent observational data and the solid line is a theoretical estimate. Masses are in solar units. (Figure adapted from Rana, *Astron. Astrophys.*, *184*, 104, 1987.)